Original

MiR-133a-3p inhibits scar formation in scalded mice and suppresses the proliferation and migration of scar derived-fibroblasts by targeting connective tissue growth factor

Abdul Razaq HIRMAN[1], Lili DU[2], Shaohang CHENG[1], Heng ZHENG[3], Linna DUO[1], Qianyu ZHAI[1] and Jing XU[1]

[1]*Department of Dermatology, Shengjing Hospital of China Medical University, No. 36, Sanhao Street, Shenyang 110004, P.R. China*
[2]*Department of Pathophysiology, College of Basic Medical Science, China Medical University, No. 77, Puhe Road, Shenbei New District, Shenyang 110122, P.R. China*
[3]*Department of Dermatology, Central Hospital Affiliated to Shenyang Medical College, No. 7, Nanqi West Road, Tiexi District, Shenyang 110024, P.R. China*

Abstract: Excessive scar formation post burn injury can cause great pain to the patients. MiR-133a-3p has been demonstrated to be anti-fibrotic in some fibrosis-related diseases. However, its possible role in scar formation has not been elucidated yet. In present study, the effect of miR-133a-3p on scar formation was investigated in a scalded model of mice. Moreover, the function of miR-133a-3p on proliferation and migration of scar-derived fibroblasts (SFs) was studied *in vitro*. It was found that miR-133a-3p was dramatically downregulated in scar tissue of scalded mice. Upregulation of miR-133a-3p by miR-133a-3p agomir obviously inhibited the scar formation in scalded mice. Histological staining showed that upregulation of miR-133a-3p attenuated the excessive deposition of collagen in scar tissue of scalded mice. *In vitro* study showed that upregulation of miR-133a-3p effectively suppressed the proliferation and migration of SFs. Besides, upregulation of miR-133a-3p attenuated the protein levels of α-smooth muscle actin (α-SMA) and collagen I, indicating that miR-133a-3p could suppress the activation of SFs. The expression of connective tissue growth factor (CTGF), a critical mediator in cell proliferation, migration and extracellular matrix (ECM) synthesis, was also downregulated by the upregulation of miR-133a-3p. Luciferase reporter assay validated that CTGF was directly targeted by miR-133a-3p. In addition, overexpression of CTGF abolished the effect of miR-133a-3p on inhibiting the proliferation, migration and activation of SFs, indicating that miR-133a-3p functioned by targeting CTGF. Therefore, miR-133a-3p might be a promising target for treating pathological scars.
Key words: connective tissue growth factor, fibroblasts, miR-133a-3p, scar formation

Introduction

The skin is the first line of defense that functions as a physical barrier to protect against the invasion of pathogenic organisms and maintain the metabolic homeostasis of human body [1]. Thermal injury caused by fire or scald can result in the disfunction of skin barrier, which may further induce severe infection and even death of burnt patients. Scald burn injury is a leading cause of burn-related emergency, especially for young children [2]. During the wound healing process of burn injury, scar formation is crucial for restoring the skin barrier. Unfortunately, due to the deposition of excessive collagen-based extracellular matrix (ECM), pathological scars

(such as hypertrophic scar and keloid) are commonly formed post-burn [3]. The formation of pathological scars can not only cause cosmetic impairment and physiological pain to the patients, but also severely affect their mental health and quality of life. To date, the mechanism under pathological scar formation is poorly understood, and the control of excessive scar formation remains to be a challenge in clinic trials.

Deposition of excessive collagen-based ECM is a typical characteristic in the formation of pathological scars, which is induced by the imbalance between the degradation and synthesis of ECM and predominantly mediated by fibroblasts [4]. In normal condition of wound healing, fibroblasts migrate into the lesions and synthesize collagen and fibronectin to promote tissue repair. Nevertheless, in pathological condition of scar formation, fibroblasts exhibit abnormally enhanced capacity of proliferation and collagen synthesis [5]. Therefore, fibroblasts are considered as potential therapeutic target in the prevention and treatment of pathological scars.

MicroRNAs (miRNAs) are small noncoding RNAs with the length of ~21–23 nucleotides, which combine with the 3' untranslated regions (UTRs) of targeted mRNAs to regulate the gene expression [6]. A wide range of miRNAs has been identified to be aberrantly expressed in scar tissues and function to control the process of pathological scar formation [7, 8]. MiR-133a-3p has been demonstrated to be anti-fibrotic in some fibrosis-related diseases, such as myocardial fibrosis and bladder fibrosis [9, 10]. More importantly, miR-133a-3p was found to be downregulated in the tissue sample of keloid patients [11]. However, its potential role in scar formation has not been elucidated yet. Connective tissue growth factor (CTGF) belongs to cellular communication network factors, which play a critical role in mediating cell proliferation, migration and synthesis of ECM [12, 13]. It has been reported that CTGF contributes to the formation of pathological scars and fibrotic skin disorders [14–16]. Moreover, CTGF is demonstrated to be a direct target of miR-133a-3p [9]. However, it is unknown that whether miR-133 could function through regulating CTGF in pathological scar formation.

In this study, the effect of miR-133a-3p on scar formation and collagen deposition was investigated in a mouse model of scald. Moreover, we explored the function of miR-133a-3p on proliferation and migration of scar-derived fibroblasts (SFs), and the underlying regulatory mechanisms.

Materials and Methods

Mice model of scald

Male BALB/c mice (8 weeks old) were adaptively raised for one week and divided into Control group, Scald group, negative control (NC) agomir group and miR-133a-3p agomir group (n=6 for each group). To establish the model of scald, mice in Scald group, NC agomir group and miR-133a-3p agomir group were anesthetized by 50 mg/kg pentobarbital sodium and shaved to expose the dorsal surface. The depth of anesthesia was evaluated by a toe-pinch test and the mice showed no foot-withdrawal response. The scald model was established based on a previously reported method with some modification [8]. Briefly, a hollow plastic pipe with the diameter of 2 cm was placed vertically onto the dorsal surface with one end closely connecting with the skin. Same volume of hot water (80°C) was then injected from the other end of the pipe and contacted with the skin for 10 s. After that, mice were flipped to get rid of the hot water. Each mouse was housed in a separate cage to avoid infection and carefully cared under a warm and comfortable environment post the operation to minimize the animal pain. Mice were monitored daily for 48 h postburn to assess the pain by observing their activity, appearance of fur and food intake. Analgesics were not required based on the observation of pain assessments. For drug administration, 250 pmol NC agomir or miR-133a-3p agomir was intradermally injected into mice skin of NC agomir group and miR-133a-3p agomir group once a week. Mice in Control and Scald groups were intradermally injected with normal saline. After 21 d, the scalded lesion was photographed and the wound areas were analyzed using Image-Pro Plus 6.0 software. Then all mice were sacrificed by injection of excessive pentobarbital sodium to collect the scar tissue. Each tissue sample was divided into two portions. One portion was fixed in 4% paraformaldehyde for histological analysis and the other portion was preserved at −80°C for quantitative real-time PCR and Western blot analysis. All animal experiments were conducted with approval of the Ethics Committee of Shengjing Hospital of China Medical University (2019PS216K).

Histological staining

The scar tissue was fixed in 4% paraformaldehyde (Sinopharm, Beijing, China) and dehydrated in ethanol gradients (70%, 80%, 90% and 100%). After embedding in paraffin, the tissue was sliced and stained by hematoxylin and eosin (H&E) or Masson's trichrome for histological analysis. Histological score was given according to a previously reported scoring system [17].

Quantitative real-time PCR

RNA sample was isolated from the scar tissue or SFs and its concentration was quantified using the UV spectrophotometer (Thermo, NanoDrop 2000, Waltham, MA, USA). The cDNA sample was obtained by reverse transcription in a PCR system (Bioneer, ExicyclerTM 96, Daejeon, Korea). The mRNA expression of miR-133a-3p and *Ctgf* was quantified by adding cDNA sample, primers, SYBR GREEN (Sigma-Aldrich, St. Louis, MO, USA) and 2×Power Taq PCR MasterMix to the PCR system. Data were calculated using $2^{-\Delta\Delta Ct}$ method and normalized to U6 or *Gapdh*. The primers were shown below:
miR-133a-3p forward, 5'-TTTGGTCCCCTTCAAC-CAGCTG-3'
miR-133a-3p reverse, 5'-GCAGGGTCCGAGGTATTC-3'
U6 forward, 5'-CGCAAGGATGACACGCAAAT-3'
U6 reverse, 5'- GCAGGGTCCGAGGTATTC-3'
Ctgf forward, 5'-TGTGAAGACATACAGGGCTAAG-3'
Ctgf reverse, 5'-ACAGTTGTAATGGCAGGCAC-3'
Gapdh forward, 5'-TGTTCCTACCCCCAATGTGTC-CGTC-3'
Gapdh reverse, 5'- CTGGTCCTCAGTGTAGCCCAA-GATG-3'

Western blot

The protein levels of α-smooth muscle actin (α-SMA), collagen I, transforming growth factor (TGF)-β1 and CTGF were determined by Western blot assay. Protein sample was extracted from the scar tissue or SFs and quantified by a BCA assay kit (Solarbio, Beijing, China). Then equal volume of sample was separated by sodium dodecyl sulfate polyacrylamide gel electrophoresis (SDS-PAGE), transferred to a PVDF membrane and blocked by 5% skimmed milk. The PVDF membrane was incubated with anti-α-SMA (Affinity, Cincinnati, OH, USA, 1:1,000 dilution), anti-collagen I (Affinity, 1:1,000 dilution), anti-TGF-β1 (Affinity, 1:1,000 dilution), anti-CTGF (Affinity, 1:1,000 dilution), anti-glyceraldehyde-3-phosphate dehydrogenase (GAPDH) (Proteintech, Rosemont, IL, USA, 1:10,000 dilution) at 4°C overnight and then treated by the secondary antibody (Solarbio, 1:3,000 dilution) at 37°C for 60 min. Target protein bands were detected by enhanced chemiluminescence reagent (Solarbio) and the optical density was analyzed by Gel-Pro-Analyzer software.

Cell culture and transfection

Scar tissue collected from a scalded mouse was washed by phosphate buffer solution (PBS) and cut into fragments. Then the tissue fragments were digested by 0.1 mg/ml type I collagenase at 37°C for 3 h, filtered by cell sieve and centrifuged to isolate the fibroblasts. The separated fibroblasts were incubated in Dulbecco's modified Eagle medium (DMEM) added with 10% FBS (Hyclone, Logan, UT, USA) at 37°C. SFs were incubated in 6-well plates and transfected with 100 pmol miR-133a-3p agomir or NC agomir using DharmaFECT transfection reagent (Horizon, Cambridge, UK).

Immunofluorescence staining

SFs were successively fixed with 4% paraformaldehyde for 15 min and permeabilized by 0.1% Triton X-100 (Beyotime, Haimen, China) for 30 min. Scar tissue slices or SFs were immersed in goat serum (Solarbio) for 15 min and incubated with anti-F4/80 (Santa Cruz, Santa Cruz, CA, USA, 1:50 diluted by PBS), anti-vimentin (Abclonal, Wuhan, China, 1:50 diluted by PBS) or anti-α-SMA (Abcam, Cambridge, UK, 1:200 diluted by PBS) at 4°C overnight. Then the tissue slices or SFs were incubated with Cy3-labeled secondary antibody (Beyotime) diluted by PBS (1:200) at room temperature for 60 min. The samples were washed by PBS to remove the residual antibodies and stained with DAPI (Aladdin, Shanghai, China). All samples were viewed by a fluorescence microscope (BX53, Olympus, Tokyo, Japan).

Cell proliferation assay

SFs (4×10^4 cells/ml) were inoculated into 96-well plates and transfected with miR-133a-3p agomir or NC agomir for 0 h, 24 h, 48 h and 72 h. At each time point, SFs were incubated with 10% cell counting kit-8 (CCK-8) (KeyGen, Nanjing, China) for 2 h at 37°C and the optical values at 450 nm were determined using a microplate reader (ELX-800, BioTex, Winooski, VT, USA).

Wound healing assay

SFs were cultured in 6-well plates supplemented with serum-free medium and 1 μg/ml mitomycin C for 1 h. The scratch was created by a pipette tip (200 μl). Then the cells were transfected with miR-133a-3p agomir or NC agomir and incubated for 24 h. The distance of migration was measured to calculate the relative wound closure.

Luciferase reporter assay

Wild type or mutant CTGF-3'UTR was constructed to the luciferase reporter plasmid. After incubating in serum-free medium for 1 h, HEK-293T cells were transfected with miR-133a-3p agomir (or NC agomir) +luciferase reporter plasmid. The firefly and Renilla luciferase activities were determined by an assay kit (KeyGen) according to the protocols 48 h later.

Statistical analysis

Data were shown as mean value ± SD. The statistical

analysis was conducted using a software (GraphPad Prism 8). Two-tailed Student's *t*-test and one-way ANOVA followed by Tukey's test were applied to assess the statistical difference. *P*<0.05 was defined to be significant.

Results

MiR-133a-3p inhibited scar formation in a mouse model of scald

To study the function of miR-133a-3p on scar formation, we established a mice model of scald and treated the scalded mice with miR-133a-3p agomir or NC agomir. After 21 d, the mRNA level of miR-133a-3p in scar tissue of Scald group was dramatically downregulated compared with Control group (Fig. 1A). Intradermal injection of miR-133a-3p agomir significantly upregulated miR-133a-3p expression in scar tissue of scalded mice while injection of NC agomir had no effect on miR-133a-3p expression. Moreover, the scalded wounds on mice of the four groups were photographed on day 0 and day 21, and the wound areas were analyzed as well. We found that the wound area was smaller in miR-133a-3p agomir group, whereas Scald group and NC agomir group showed larger wound areas on the scalded lesions (Figs. 1B and C). These results indicated that upregulation of miR-133a-3p could inhibited scar formation of scalded mice.

MiR-133a-3p inhibited the deposition of collagen in scar tissue of scalded mice

Histological staining was further performed to display the pathological changes in scar tissue of the four groups after 21 d. Comparing to the skin tissue of normal mice, the scalded tissue of mice in Scald group showed thickened epidermis and dermis, as well as irregular and dense collagen deposition (Fig. 2A). Scald group also had a high histological score. Treating with miR-133a-3p agomir alleviated the pathological changes in scalded mice. In addition, the histological score was much lower in miR-133a-3p agomir group than in NC agomir group. Moreover, immunofluorescence staining for F4/80 was conducted to evaluate the infiltration of macrophages in the scar tissue of mice. We found that Scald group and NC agomir group showed many macrophages in the scar tissue, indicating that scald induced severe inflammation in the skin tissue of mice (Fig. 2B). By contrast, treating with miR-133a-3p agomir obviously reduced the infiltration of macrophages in the scar tissue. Furthermore, immunofluorescence staining for vimentin and α-SMA was conducted to indicate the proliferation of fibroblasts. As expected, much more vimentin-positive and α-SMA-positive cells was observed in Scald group and NC agomir group, indicating the abnormal proliferation of fibroblasts in the scar tissue of mice (Fig. 2B). However, miR-133a-3p agomir group showed less vimentin-positive and α-SMA-positive cells in the scar tissue, demonstrating that miR-133a-3p could inhibited the proliferation of fibroblasts.

In addition, we determined the levels of ECM-related proteins (α-SMA and collagen I) in skin tissue of these mice. The relative expression of both α-SMA and collagen I were dramatically elevated in Scald group compared with Control group (Figs. 3A–C). On the contrary, injection of miR-133a-3p agomir effectively downregu-
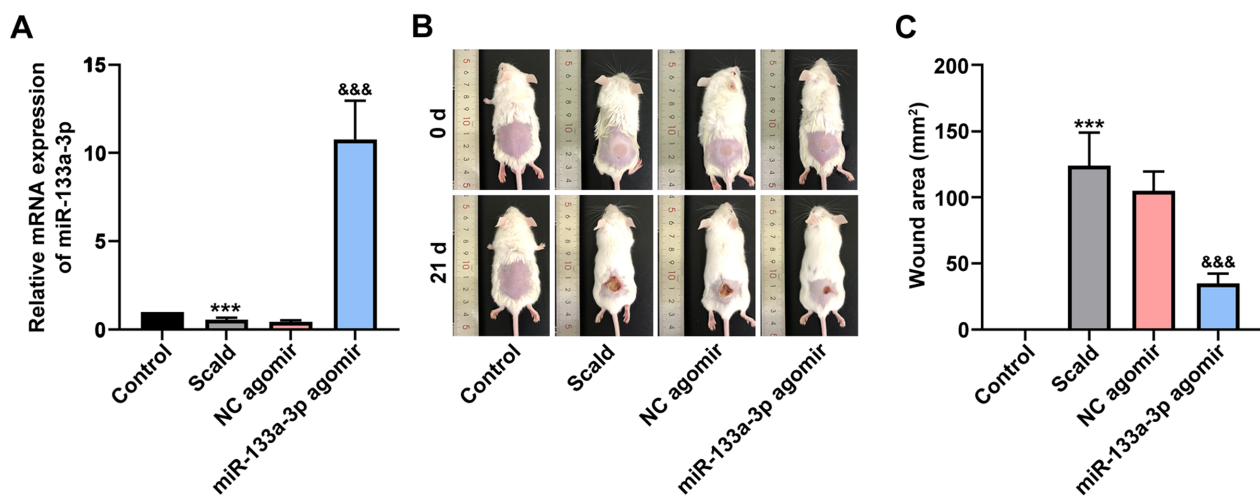

Fig. 1. MiR-133a-3p inhibited scar formation in a mouse model of scald. The scalded mice were treated with miR-133a-3p agomir or negative control (NC) agomir. (A) The mRNA level of miR-133a-3p in scar tissue of mice analyzed by real-time PCR. (B) Representative images of wounds photographed at 0 d and 21 d on non-treated mice and mice treated with miR-133a-3p agomir of NC agomir. (C) The wound area of mice analyzed after treating for 21 d. Data were shown as mean value ± SD (n=6). ****P*<0.001, versus Control group. &&&*P*<0.001, versus NC agomir group.

lated the protein levels of α-SMA and collagen I in the scalded tissue of mice, demonstrating the function of miR-133a-3p on inhibiting the excessive deposition of collagen in scar tissue of scalded mice. More interestingly, Scald group expressed significantly higher TGF-β1 and CTGF in the scalded tissue, while treating with miR-133a-3p agomir attenuated the expression of these fibrosis-related proteins (Figs. 3D and E). These findings suggested the potential antifibrotic effect of miR-133a-3p.

MiR-133a-3p suppressed the proliferation and migration of SFs

Furthermore, the effect of miR-133a-3p was investigated on SFs since fibroblasts play a dominant role in mediating pathological scar formation. To identify the separated fibroblasts from scar tissue, immunofluorescence staining for vimentin was conducted. The representative images showed positive vimentin expression in separated cells (Fig. 4A), demonstrating that the fibroblasts were successfully extracted from scar tissue of scalded mice. The SFs were then transfected with miR-133a-3p agomir or NC agomir. To verify the efficiency of transfection, miR-133a-3p expression was determined by real-time PCR. It was shown that treating with miR-133a-3p agomir greatly enhanced miR-133a-3p expression in SFs (Fig. 4B). Cell proliferation assay was conducted to evaluate the proliferative activity of control SFs and SFs treated with miR-133a-3p agomir or NC
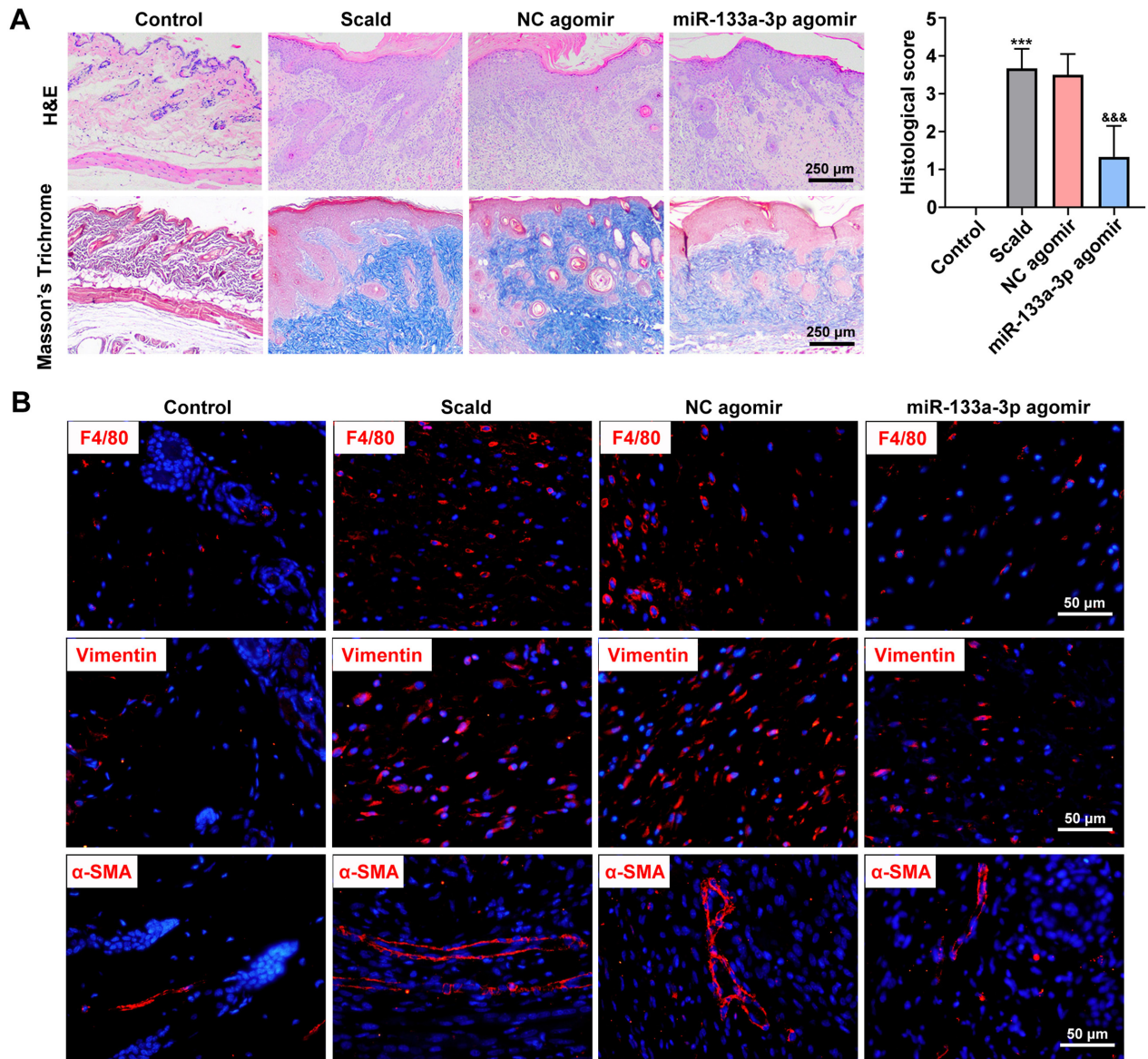

Fig. 2. MiR-133a-3p suppressed the pathological changes in scar tissue of scalded mice. (A) The images of hematoxylin and eosin (H&E) and Masson's trichrome staining for scar tissue of the mice and score for histological analysis. (B) The images of immunofluorescence staining for F4/80, vimentin and α-smooth muscle actin (α-SMA) in scar tissue of the mice. Data were shown as mean value ± SD (n=6). ***$P<0.001$, versus Control group. &&&$P<0.001$, versus NC agomir group.
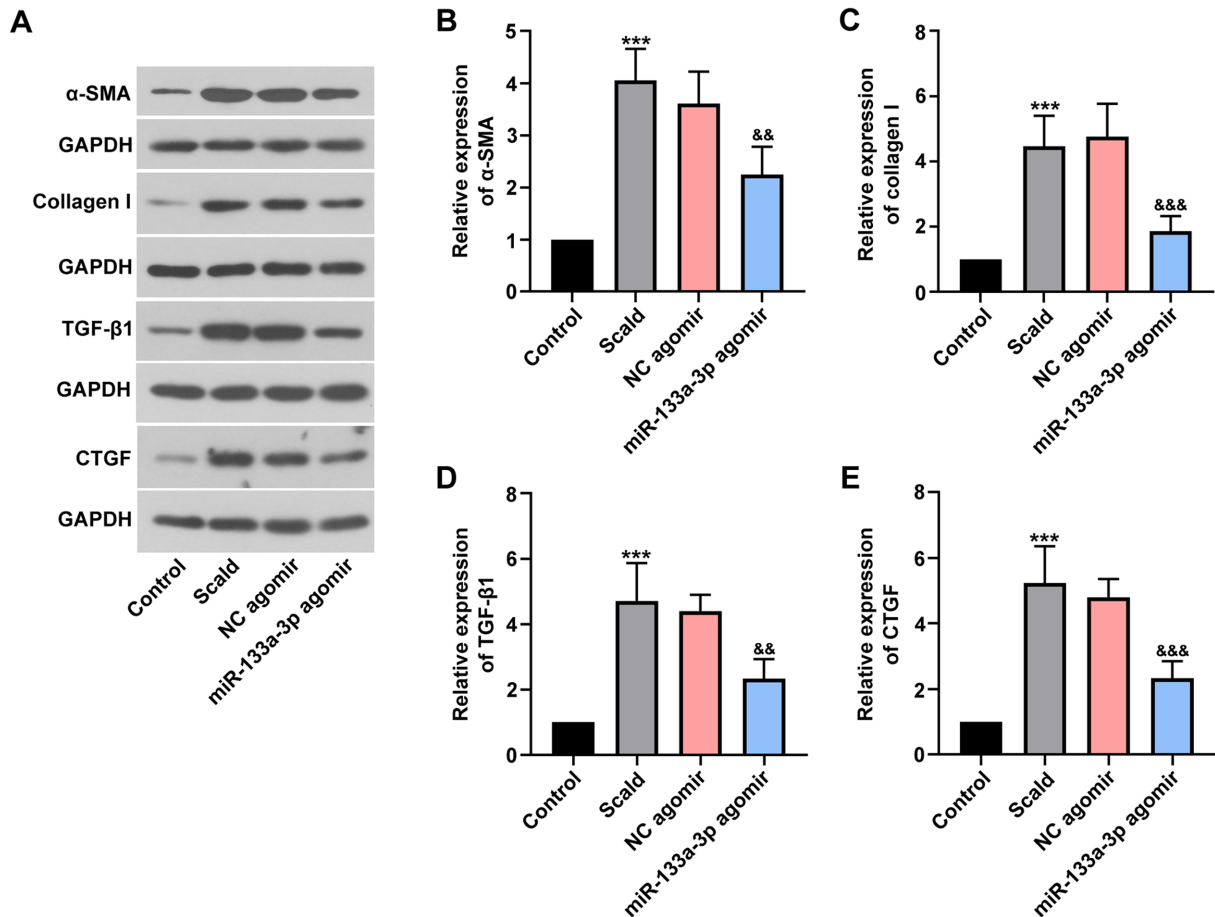
Fig. 3. MiR-133a-3p attenuated the expression of fibrosis-related proteins in scar tissue of scalded mice. (A) Western blot analysis for α-smooth muscle actin (α-SMA), collagen I, transforming growth factor (TGF)-β1 and connective tissue growth factor (CTGF). The relative expression of (B) α-SMA, (C) collagen I, (D) TGF-β1 and (E) CTGF. Data were shown as mean value ± SD (n=6). ***$P<0.001$, versus Control group. &&$P<0.01$, &&&$P<0.001$, versus NC agomir group.

agomir. The OD values were significantly decreased in SFs of miR-133a-3p agomir group after incubating for 24 h, 48 h and 72 h (Fig. 4C). This result indicated that upregulation of miR-133a-3p could suppress the proliferation of SFs. We next investigated the migration of SFs in the three groups by wound healing assay. As expected, control SFs showed strong capacity of migration and the relative wound closure reached 54% after incubating for 24 h (Figs. 4D and E). However, SFs transfected with miR-133a-3p showed weakened capacity of migration compared to SFs transfected with NC agomir. We also determined the protein levels of α-SMA and collagen I in these SFs. Result showed that α-SMA and collagen I were dramatically downregulated in miR-133a-3p agomir group, comparing to NC agomir group (Figs. 4F–H). Therefore, it was indicated that miR-133a-3p suppressed the proliferation and migration of SFs.

CTGF was a direct target of miR-133a-3p

MiR-133a-3p was predicted to combinate with wild type CTGF-3'UTR (Fig. 5A). The relationship between CTGF and miR-133a-3p was verified by luciferase reporter assay. The relative luciferase activity in CTGF-3'UTR (WT)+miR-133a-3p agomir group was dramatically decreased compared with CTGF-3'UTR (WT)+NC agomir (Fig. 5B). Moreover, the mutation of CTGF-3'UTR abolished its combination with miR-133a-3p, implying that miR-133a-3p combined with wild type CTGF-3'UTR at the predicted binding site. We determined the expression of CTGF in SFs treated with miR-133a-3p agomir or NC agomir. It was shown that CTGF expression in mRNA and protein levels were both remarkably downregulated in miR-133a-3p agomir group (Figs. 5C–E), indicating that upregulation of miR-133a-3p suppressed the expression of CTGF. Therefore, it could be demonstrated that CTGF was directly targeted by miR-133a-3p.

MiR-133a-3p inhibited the proliferation and migration of SFs by targeting CTGF

To further explore whether miR-133a-3p functioned through regulating CTGF, SFs were transfected with
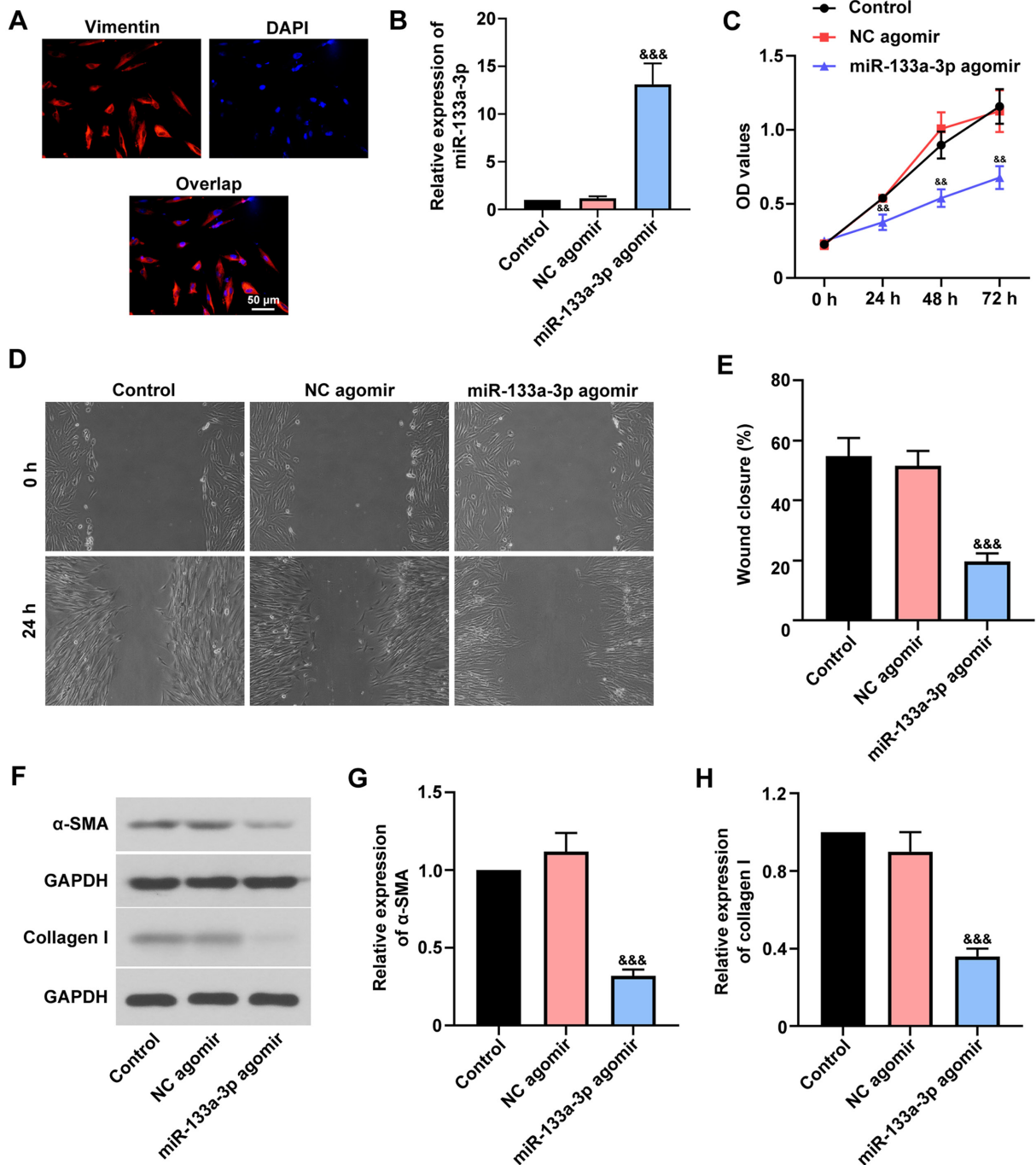
Fig. 4. MiR-133a-3p suppressed the proliferation and migration of scar-derived fibroblasts (SFs). SFs were treated with miR-133a-3p agomir or negative control (NC) agomir. (A) The images of immunofluorescence staining for vimentin in SFs. (B) The relative mRNA level of miR-133a-3p in non-treated SFs and SFs transfected with miR-133a-3p agomir or NC agomir. (C) Cell counting kit-8 (CCK-8) assay for evaluation of cell proliferation. (D) Representative images of wound healing assay. (E) The relative wound closure analyzed after incubating for 24 h. (F) Western blot analysis for α-smooth muscle actin (α-SMA) and collagen I in SFs. The relative protein expression of (G) α-SMA and (H) collagen I in SFs. Data were shown as mean value ± SD (n=3). &&P<0.01, &&&P<0.001, versus NC agomir group.

miR-133a-3p agomir and CTGF overexpression vector (or empty vector as control). Transfecting with CTGF overexpression vector could significantly increase the expression of CTGF as analyzed by real-time PCR (Fig. 6A), verifying the efficiency of transfection. We then tested the proliferation of SFs transfected with miR-133a-5p agomir and CTGF overexpression vector by CCK-8 assay. The result showed that SFs transfected with miR-133a-3p agomir and CTGF overexpression vector had greatly enhanced capacity of proliferation than SFs transfected with miR-133a-3p agomir and empty vector (Fig. 6B). Therefore, it was indicated that
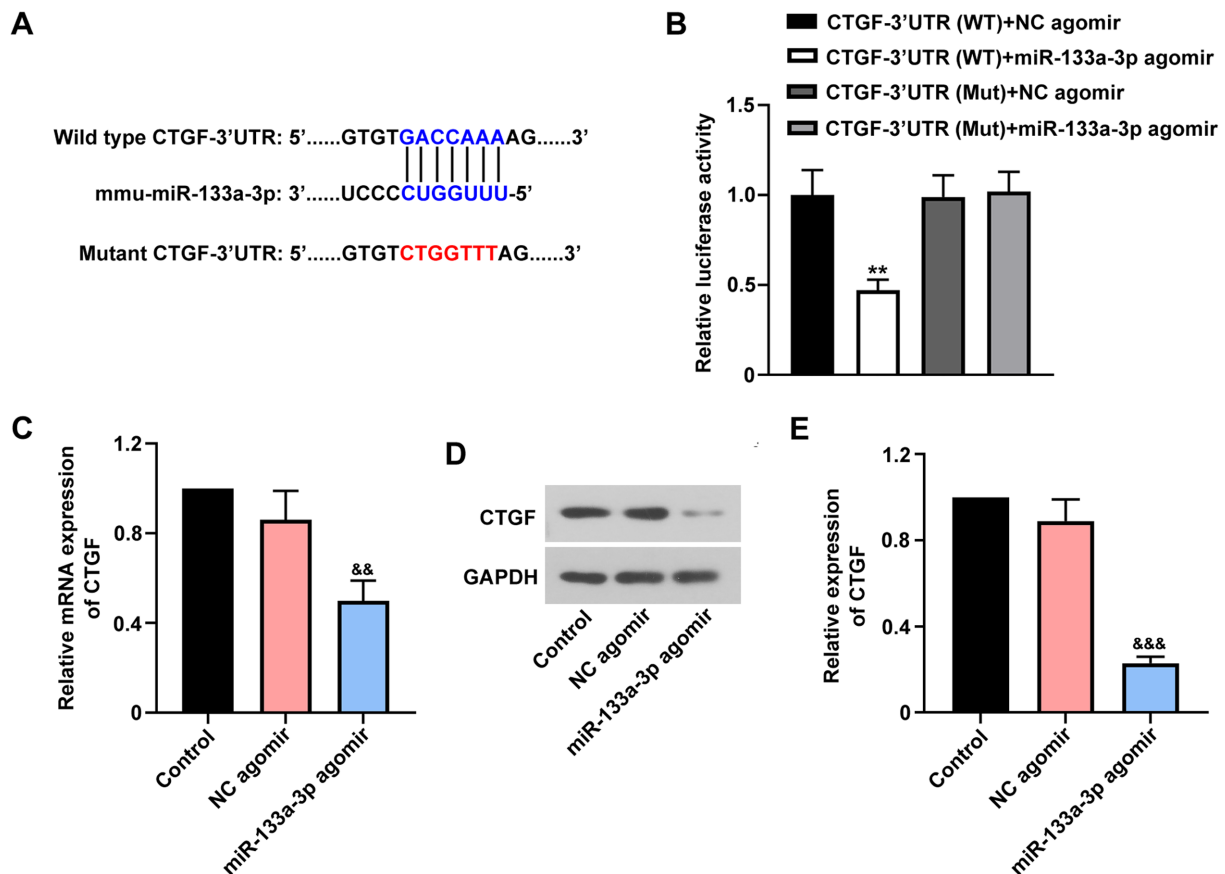
Fig. 5. Connective tissue growth factor (CTGF) was a direct target of miR-133a-3p. (A) The mutant site of CTGF-3' untranslated region (UTR) and the potential binding site of miR-133a-5p with wild type CTGF-3'UTR. (B) Relative luciferase activity assessed by luciferase reporter assay. (C) The relative mRNA expression of *Ctgf* in non-treated scar-derived fibroblasts (SFs) and SFs transfected with miR-133a-3p agomir or negative control (NC) agomir. (D) Western blot analysis for CTGF in SFs. (E) The relative protein expression of CTGF in SFs. Data were shown as mean value ± SD (n=3). **$P<0.01$, versus CTGF-3'UTR (WT)+NC agomir group. &&$P<0.01$, &&&$P<0.001$, versus NC agomir group.

the function of miR-133a-3p on inhibiting proliferation was abolished by CTGF overexpression. The capacity of migration was also analyzed in the two groups by wound healing assay. SFs co-transfected with miR-133a-3p agomir and CTGF overexpression vector showed obviously enhanced capacity of migration (Figs. 6C and D), which suggested that the function of miR-133a-3p on inhibiting migration was abolished by CTGF over-expression as well. We then determined the protein levels of α-SMA and collagen I in these cells by Western blot. Not surprisingly, both α-SMA and collagen I expression was much higher in miR-133a-3p agomir + CTGF vector group (Figs. 6E and F). Thus, it was validated that miR-133a-3p functioned by targeting CTGF.

Disccusion

Excessive scar formation post-burn can cause great physiological and psychological trauma to the patients. Although advanced technology and multiple drugs have been applied for improving the scar formation in clinic,

there is no satisfactory therapeutic methods to treat pathological scars at present. Recently, a large number of miRNAs has been recognized to play important roles in the pathogenesis of excessive scar formation [8, 18]. Previous studies have made great effort on elucidating the effect of some miRNAs on scar formation and exploring the potential underlying mechanisms [19, 20]. Nevertheless, the role of miR-133a-3p in scar formation is not fully clarified at present. In this study, we aimed to investigate the potential role of miR-133a-3p in scar formation and its effect on the proliferation and migration of SFs.

Scald burn injury is a leading cause of burn-related emergency, especially for young children [21, 22]. In the present study, a mouse model of scald was established, and we found that miR-133a-3p expression was noticeably decreased in the scar tissue of mice in Scald group. Treating with miR-133a-3p agomir significantly enhanced miR-133a-3p expression in scar tissue of scalded mice. It was also found that the scald resulted in severe wound injury and scar formation on the skin surface of mice in Scald group while upregulation of miR-133a-
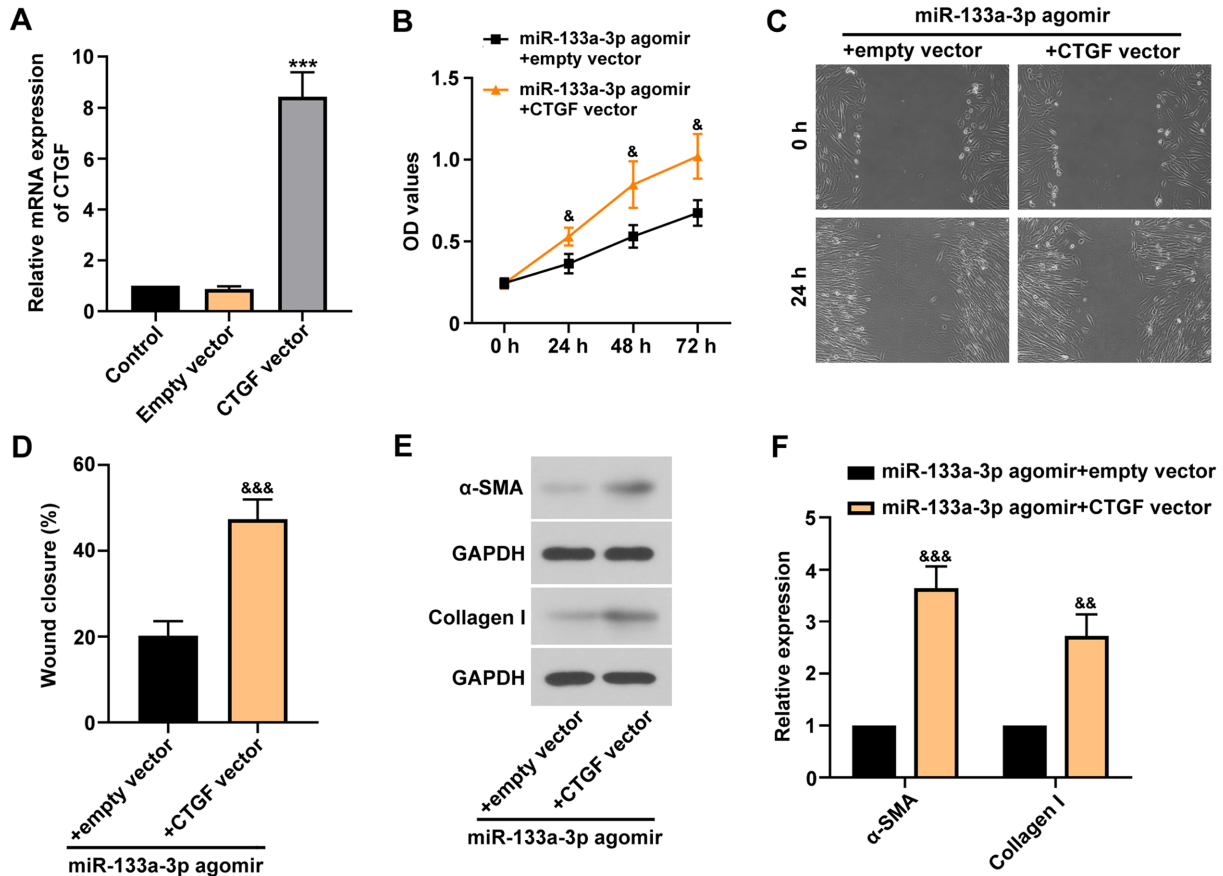
Fig. 6. MiR-133a-3p suppressed the proliferation and migration of scar-derived fibroblasts (SFs) through regulating connective tissue growth factor (CTGF). SFs were transfected with miR-133a-3p agomir and CTGF overexpression vector (or empty vector as control). (A) The relative mRNA expression of *Ctgf* in non-treated SFs and SFs transfected with CTGF overexpression vector or empty vector. (B) Cell counting kit-8 (CCK-8) assay for evaluating cell proliferation. (C) Representative images of wound healing assay for evaluating cell migration. (D) The relative wound closure analyzed after incubating for 24 h. (E) Western blot analysis for α-smooth muscle actin (α-SMA) and collagen I in SFs. (F) The relative protein levels of α-SMA and collagen I in SFs. Data were shown as mean value ± SD (n=3). ***$P<0.001$, versus Empty vector group. &$P<0.05$, &&$P<0.01$, &&&$P<0.001$, versus miR-133a-3p agomir+empty vector group.

3p effectively reduced the scar formation on scalded mice. This result revealed the possible effect of miR-133a-3p on inhibiting scar formation. Analysis for histological and immunofluorescence staining indicated that the structure of epidermis and dermis was destroyed by scald, which caused severe inflammatory cell infiltration and collagen deposition. This observation was in coincidence with scald-induced pathological changes reported in previous research [8]. More importantly, upregulation of miR-133a-3p attenuated the deposition of collagen in scar tissue of scalded mice.

Excessive scar formation is usually characterized by dermal hyperplasia, excessive deposition of collagen-based ECM and fibrosis [23]. The excessive deposition of ECM is a major pathological feature in scar formation and α-SMA and collagen I are important ECM-related proteins [24]. In this study, the levels of α-SMA and collagen I was dramatically elevated in scar tissue of model mice and downregulated by the upregulation of

miR-133a-3p. Thus, it was suggested that miR-133a-3p might function to inhibit excessive ECM synthesis in scar tissue of mice. The function of miR-133a on collagen synthesis has been reported in some fibrosis-related diseases. Roderburg *et al.* showed that overexpression of miR-133a resulted in the downregulation of collagens in hepatic stellate cells [25]. Castoldi *et al.* demonstrated that miR-133a-3p modulated myocardial remodeling by targeting collagen 1A1 [10]. In this study, miR-133a-3p also showed inhibitory effect on collagen synthesis through attenuating the level of collagen I in the scar tissue of scalded mice. More interestingly, we found that the expression of fibrosis-related TGF-β1 and CTGF was dramatically upregulated in the scar tissue of scalded mice. TGF-β1 has been identified as a dominant regulator in multiple fibrosis-related diseases, such as renal fibrosis and liver fibrosis [26]. Moreover, TGF-β1 also plays a profibrotic role in the formation of pathological scars through promoting fibroblasts proliferation and

transdifferentiation [7, 27]. CTGF is a downstream mediator of TGF-β1, which stimulates cell proliferation and synthesis of ECM in connective tissues [28]. It has been documented that miR-133a-3p negatively regulates the expression of TGF-β1 and CTGF [29, 30]. Therefore, we speculated that miR-133a-3p might inhibit the excessive scar formation in scaled mice through regulating TGF-β1 and CTGF.

Since the deposition of collagen-based ECM is predominantly mediated by fibroblasts, we separated the SFs from scalded mice and investigated the potential function of miR-133a-3p on the proliferation and migration of SFs. Previous studies demonstrated that SFs possessed strongly enhanced capacity of proliferation and migration, which created favorable conditions for them to promote excessive scar formation [31, 32]. Our study showed that upregulation of miR-133a-3p greatly suppressed the proliferation and migration of SFs. In addition, upregulation of miR-133a-3p effectively decreased the protein levels of α-SMA and collagen I in SFs. α-SMA is a marker of myofibroblasts, which derive from activated fibroblasts and exhibit stronger ability in collagen synthesis [33]. The formation of myofibroblasts usually leads to overabundant deposition of ECM during wound repairing and further induces the pathological scar formation [5, 34, 35]. Therefore, it was implicated that miR-133a-3p suppressed the activation of SFs.

To further exploring the potential mechanism, we determined the expression of CTGF in SFs. CTGF is known to be critical in regulating cell adhesion, proliferation and migration, as well as ECM deposition and tissue remodeling [36]. The overexpression of CTGF is common in fibrosis-related diseases and tightly associated with excessive scar formation [37]. In our study, the mRNA and protein levels of CTGF were noticeably downregulated in SFs treated with miR-133a-3p agomir, suggesting that miR-133a-3p functioned to inhibit the expression of CTGF. Besides, the result of luciferase reporter assay demonstrated that CTGF was directly targeted by miR-133a-3p. To investigate whether miR-133a-3p functioned through regulating CTGF, SFs were transfected with miR-133a-3p and CTGF overexpression vector. Interestingly, the function of miR-133a-3p on inhibiting proliferation and migration was abolished by overexpression of CTGF. In addition, the overexpression of CTGF also resulted in the upregulation of α-SMA and collagen I in SFs. These results implicated that miR-133a-3p functioned to inhibit the proliferation, migration and activation of SFs by targeting CTGF. From the findings above, both CTGF and TGF-β1 expression levels were upregulated in scald tissue, accompanied with a downregulation of miR-133a-3p. CTGF has been re-

ported to be a downstream mediator of TGF-β1 [38, 39]. It is demonstrated that CTGF is required for TGF-β1-induced fibrosis [40]. CTGF was showed to facilitate the TGF-β1 signaling. Besides, TGF-β1 was identified to induce miR-133a-3p expression, which functioned as an anti-fibrotic factor and a feed-back negative regulator of TGF-β1 profibrogenic signaling [41]. Therefore, miR-133a-3p might have effects on downregulation of CTGF, not only by binding to 3'UTR of CTGF gene, but also indirect effects through downregulation TGF-β1 as an upstream mediator. The underlying molecular mechanisms of regulation among miR-133a-3p, TGF-β1, and CTGF deserve further investigation.

In summary, miR-133a-3p was significantly downregulated in scar tissue of scalded mice and upregulation of miR-133a-3p inhibited scar formation and excessive collagen deposition in scalded mice. Moreover, miR-133a-3p functioned to suppress the proliferation, migration and activation of SFs through regulating CTGF. Therefore, miR-133a-3p might be a promising target for preventing excessive scar formation.

Conflict of Interests

The authors declare that they have no conflict of interests.

Acknowledgments

References

1. Grice EA, Segre JA. The skin microbiome. Nat Rev Microbiol. 2011; 9: 244–253. [Medline] [CrossRef]
2. Yeoh C, Nixon JW, Dickson W, Kemp A, Sibert JR. Patterns of scald injuries. Arch Dis Child. 1994; 71: 156–158. [Medline] [CrossRef]
3. Xue M, Jackson CJ. Extracellular matrix reorganization during wound healing and its impact on abnormal scarring. Adv Wound Care (New Rochelle). 2015; 4: 119–136. [Medline] [CrossRef]
4. Darby IA, Laverdet B, Bonté F, Desmoulière A. Fibroblasts and myofibroblasts in wound healing. Clin Cosmet Investig Dermatol. 2014; 7: 301–311. [Medline]
5. Sarrazy V, Billet F, Micallef L, Coulomb B, Desmoulière A. Mechanisms of pathological scarring: role of myofibroblasts and current developments. Wound Repair Regen. 2011; 19:(Suppl 1): s10–s15. [Medline] [CrossRef]
6. Bushati N, Cohen SM. microRNA functions. Annu Rev Cell Dev Biol. 2007; 23: 175–205. [Medline] [CrossRef]
7. Liu Y, Li Y, Li N, Teng W, Wang M, Zhang Y, et al. TGF-β1 promotes scar fibroblasts proliferation and transdifferentiation via up-regulating MicroRNA-21. Sci Rep. 2016; 6: 32231. [Medline] [CrossRef]
8. Guo J, Lin Q, Shao Y, Rong L, Zhang D. miR-29b promotes

skin wound healing and reduces excessive scar formation by inhibition of the TGF-β1/Smad/CTGF signaling pathway. Can J Physiol Pharmacol. 2017; 95: 437–442. [Medline] [Cross-Ref]

9. Duan LJ, Qi J, Kong XJ, Huang T, Qian XQ, Xu D, et al. MiR-133 modulates TGF-β1-induced bladder smooth muscle cell hypertrophic and fibrotic response: implication for a role of microRNA in bladder wall remodeling caused by bladder outlet obstruction. Cell Signal. 2015; 27: 215–227. [Medline] [CrossRef]

10. Castoldi G, Di Gioia CR, Bombardi C, Catalucci D, Corradi B, Gualazzi MG, et al. MiR-133a regulates collagen 1A1: potential role of miR-133a in myocardial fibrosis in angiotensin II-dependent hypertension. J Cell Physiol. 2012; 227: 850–856. [Medline] [CrossRef]

11. Zhong L, Bian L, Lyu J, Jin H, Liu Z, Lyu L, et al. Identification and integrated analysis of microRNA expression profiles in keloid. J Cosmet Dermatol. 2018; 17: 917–924. [Medline] [CrossRef]

12. Shi-Wen X, Leask A, Abraham D. Regulation and function of connective tissue growth factor/CCN2 in tissue repair, scarring and fibrosis. Cytokine Growth Factor Rev. 2008; 19: 133–144. [Medline] [CrossRef]

13. Abreu JG, Ketpura NI, Reversade B, De Robertis EM. Connective-tissue growth factor (CTGF) modulates cell signalling by BMP and TGF-β. Nat Cell Biol. 2002; 4: 599–604. [Medline] [CrossRef]

14. Khoo YT, Ong CT, Mukhopadhyay A, Han HC, Do DV, Lim IJ, et al. Upregulation of secretory connective tissue growth factor (CTGF) in keratinocyte-fibroblast coculture contributes to keloid pathogenesis. J Cell Physiol. 2006; 208: 336–343. [Medline] [CrossRef]

15. Sisco M, Kryger ZB, O'Shaughnessy KD, Kim PS, Schultz GS, Ding XZ, et al. Antisense inhibition of connective tissue growth factor (CTGF/CCN2) mRNA limits hypertrophic scarring without affecting wound healing in vivo. Wound Repair Regen. 2008; 16: 661–673. [Medline] [CrossRef]

16. Chujo S, Shirasaki F, Kondo-Miyazaki M, Ikawa Y, Takehara K. Role of connective tissue growth factor and its interaction with basic fibroblast growth factor and macrophage chemoattractant protein-1 in skin fibrosis. J Cell Physiol. 2009; 220: 189–195. [Medline] [CrossRef]

17. Domergue S, Bony C, Maumus M, Toupet K, Frouin E, Rigau V, et al. Comparison between stromal vascular fraction and adipose mesenchymal stem cells in remodeling hypertrophic scars. PLoS One. 2016; 11: e0156161. [Medline] [CrossRef]

18. Babalola O, Mamalis A, Lev-Tov H, Jagdeo J. The role of microRNAs in skin fibrosis. Arch Dermatol Res. 2013; 305: 763–776. [Medline] [CrossRef]

19. Wu X, Li J, Yang X, Bai X, Shi J, Gao J, et al. miR-155 inhibits the formation of hypertrophic scar fibroblasts by targeting HIF-1α via PI3K/AKT pathway. J Mol Histol. 2018; 49: 377–387. [Medline] [CrossRef]

20. Kashiyama K, Mitsutake N, Matsuse M, Ogi T, Saenko VA, Ujifuku K, et al. miR-196a downregulation increases the expression of type I and III collagens in keloid fibroblasts. J Invest Dermatol. 2012; 132: 1597–1604. [Medline] [CrossRef]

21. Feldman KW, Schaller RT, Feldman JA, McMillon M. Tap water scald burns in children. 1997. Inj Prev. 1998; 4: 238–242. [Medline] [CrossRef]

22. Dissanaike S, Rahimi M. Epidemiology of burn injuries: highlighting cultural and socio-demographic aspects. Int Rev Psychiatry. 2009; 21: 505–511. [Medline] [CrossRef]

23. Tuan TL, Nichter LS. The molecular basis of keloid and hypertrophic scar formation. Mol Med Today. 1998; 4: 19–24. [Medline] [CrossRef]

24. Varkey M, Ding J, Tredget EE. Differential collagen-glycosaminoglycan matrix remodeling by superficial and deep dermal fibroblasts: potential therapeutic targets for hypertrophic scar. Biomaterials. 2011; 32: 7581–7591. [Medline] [Cross-Ref]

25. Roderburg C, Luedde M, Vargas Cardenas D, Vucur M, Mollnow T, Zimmermann HW, et al. miR-133a mediates TGF-β-dependent derepression of collagen synthesis in hepatic stellate cells during liver fibrosis. J Hepatol. 2013; 58: 736–742. [Medline] [CrossRef]

26. Meng XM, Nikolic-Paterson DJ, Lan HY. TGF-β: the master regulator of fibrosis. Nat Rev Nephrol. 2016; 12: 325–338. [Medline] [CrossRef]

27. Shi JH, Guan H, Shi S, Cai WX, Bai XZ, Hu XL, et al. Protection against TGF-β1-induced fibrosis effects of IL-10 on dermal fibroblasts and its potential therapeutics for the reduction of skin scarring. Arch Dermatol Res. 2013; 305: 341–352. [Medline] [CrossRef]

28. Penn JW, Grobbelaar AO, Rolfe KJ. The role of the TGF-β family in wound healing, burns and scarring: a review. Int J Burns Trauma. 2012; 2: 18–28. [Medline]

29. Huang Y, Wang Y, Lin L, Wang P, Jiang L, Liu J, et al. Overexpression of miR-133a-3p inhibits fibrosis and proliferation of keloid fibroblasts by regulating IRF5 to inhibit the TGF-β/Smad2 pathway. Mol Cell Probes. 2020; 52: 101563. [Medline] [CrossRef]

30. Yao L, Zhou B, You L, Hu H, Xie R. LncRNA MIAT/miR-133a-3p axis regulates atrial fibrillation and atrial fibrillation-induced myocardial fibrosis. Mol Biol Rep. 2020; 47: 2605–2617. [Medline] [CrossRef]

31. Li H, Yang L, Zhang Y, Gao Z. Kaempferol inhibits fibroblast collagen synthesis, proliferation and activation in hypertrophic scar via targeting TGF-β receptor type I. Biomed Pharmacother. 2016; 83: 967–974. [Medline] [CrossRef]

32. Xiao YY, Fan PJ, Lei SR, Qi M, Yang XH. MiR-138/peroxisome proliferator-activated receptor β signaling regulates human hypertrophic scar fibroblast proliferation and movement in vitro. J Dermatol. 2015; 42: 485–495. [Medline] [Cross-Ref]

33. Nedelec B, Shankowsky H, Scott PG, Ghahary A, Tredget EE. Myofibroblasts and apoptosis in human hypertrophic scars: the effect of interferon-α2b. Surgery. 2001; 130: 798–808. [Medline] [CrossRef]

34. Shin D, Minn KW. The effect of myofibroblast on contracture of hypertrophic scar. Plast Reconstr Surg. 2004; 113: 633–640. [Medline] [CrossRef]

35. Desmoulière A, Chaponnier C, Gabbiani G. Tissue repair, contraction, and the myofibroblast. Wound Repair Regen. 2005; 13: 7–12. [Medline] [CrossRef]

36. Lipson KE, Wong C, Teng Y, Spong S. CTGF is a central mediator of tissue remodeling and fibrosis and its inhibition can reverse the process of fibrosis. Fibrogenesis Tissue Repair. 2012; 5:(Suppl 1): S24. [Medline] [CrossRef]

37. Ihn H. Pathogenesis of fibrosis: role of TGF-β and CTGF. Curr Opin Rheumatol. 2002; 14: 681–685. [Medline] [Cross-Ref]

38. Nakai K, Karita S, Igarashi J, Tsukamoto I, Hirano K, Kubota Y. COA-Cl prevented TGF-β1-induced CTGF expression by Akt dephosphorylation in normal human dermal fibroblasts, and it attenuated skin fibrosis in mice models of systemic sclerosis. J Dermatol Sci. 2019; 94: 205–212. [Medline] [Cross-Ref]

39. Jeon KI, Phipps RP, Sime PJ, Huxlin KR. Inhibitory effects of PPARγ ligands on TGF-β1-induced CTGF expression in cat corneal fibroblasts. Exp Eye Res. 2015; 138: 52–58. [Medline] [CrossRef]

40. Sharma M, Radhakrishnan R. CTGF is obligatory for TGF-β1 mediated fibrosis in OSMF. Oral Oncol. 2016; 56: e10–e11. [Medline] [CrossRef]

41. Wei P, Xie Y, Abel PW, Huang Y, Ma Q, Li L, et al. Transforming growth factor (TGF)-β1-induced miR-133a inhibits myofibroblast differentiation and pulmonary fibrosis. Cell Death Dis. 2019; 10: 670. [Medline] [CrossRef]